Numerical simulation of flow field coupling with electric field for leakage current particulate matter sensor

Guoliang Chu[1,*], *Huimin* Lv[1], *Shengyao* Shi[2], *Tianxiang* Li[2], and *Dong* Tang[2]

[1]Weichai Power Co., Ltd., State key laboratory of internal combustion engine reliability, Weifang, Shandong Province, 261061, China
[2]Department of Automotive Traffic Engineering, Jiangsu University, Zhenjiang 212013, China

Abstract. With the diesel particulate filter more and more widely applied on engine, the particulate matter (PM) sensor is used to detect malfunctions of diesel particulate filter (DPF) in on board diagnostics (OBD). This paper focused on the new leakage current particulate matter sensor, which has more practical significance. The electric field and flow field were simulated by the COMSOL Multihysics, and the influence rules of sensor electrode parameters on the electric field and flow field were analyzed. The dynamic characteristics of particulate matters with different charges was studied. The simulation results showed that the average electric field strength was higher with higher electrode voltage and larger electrode spacing, which made the motion trend of charged particulate matter to electrodes more obvious. The decrease of electrode spacing or the increase of electrode length made the exhaust flow more stable, and the motion trend of charged particulate matters to electrodes is more obvious with the increase of electrode length. It was concluded that the flow of the exhaust and particulate matter was in good condition when the electrode spacing was 12.5mm, the electrode length is 12.5mm and the electrode voltage ranged between 1000V and 1500V.

Keywords: Particulate matter sensor, Electric field, Flow field, Numerical simulation.

1 Introduction

In recent decades, with the rapid development of my country's economy, diesel engines have been widely used in various fields such as construction machinery, agricultural machinery, and transportation [1,2]. However, diesel engine exhaust has more particulate matter, and its impact on the environment is mainly manifested in the formation of haze weather. Regarding the emission of diesel particulate matter, the emission regulations formulated by countries all over the world have become increasingly stringent [3-5]. In order to meet the emission limit requirements for particulate matter in the emission regulations, a particulate matter trap will be applied to the after-treatment system. In order to ensure the

* Corresponding author: cegel@sina.com

reliable regeneration of the DPF and detect the concentration of exhaust particulate matter, a particulate matter sensor that can detect the concentration of particulate matter in real time needs to be installed downstream of the DPF. The resistive and capacitive particulate matter sensors jointly developed by the German Bosch company and the Japanese NTK company use multilayer ceramic technology to convert the resistance and capacitance values into the concentration of particulate matter [6,7]; The charge current difference particle sensor developed by the Picasso company of Finland is equipped with a corona charger in the sensor Faraday cup, and the electrometer in the sensor is used to measure the current difference between the Faraday cup before and after charging to obtain the particle concentration [8]; The dual-electrode particle sensor developed by Emisense and Teas University uses the principle of natural charge deposition to monitor the concentration of particles in engine exhaust[9,10];K. Almendingo et al. proposed a particle sensor for measuring particle accumulation and charge loss, using an integrating capacitor to integrate the current pulses from the charge transfer from the sensor electrode of the particle structure [11]. However, the research on the prototype mechanism of the particulate matter sensor is not deep enough. This article takes a leakage current particulate sensor as the research object to simulate the electric field and flow field distribution in the sensor to explore the dynamic characteristics of the particles in the leakage current particle sensor.

2 Basic introduction of leakage current particle sensor

The design principle of the new leakage current type particulate matter sensor comes from a kind of agglomeration and charge loss sensor used to measure particulate matter by the American Emisons Technology Co., Ltd. Its structural design is based on the Venturi tube principle. When the exhaust gas flows through the high-voltage electric field between the high-voltage electrode and the conductive shell, the charged particles in the exhaust move under the action of the high-voltage electric field, forming a leakage between the conductive housing and the high-voltage electrode.The leakage current between the electrodes changes with the change of the particulate matter concentration in the exhaust. The leakage current generated by the movement of the particulate matter between the electrodes can be collected to obtain the exhaust particulate matter concentration.

This paper uses multiphysics coupling simulation software to simulate the electric field distribution and flow field distribution in the sensor, changing the electrode spacing, electrode length and electrode voltage to explore the influence of the sensor electrode structure parameters on the electric field and flow field distribution in the sensor.

3 The numerical model

According to the actual three-dimensional structure of the leakage current particulate sensor, the 3D geometric model of the particulate sensor installed on the exhaust pipe is drawn using the drawing module that comes with COMOSL, according to the principle of single variable, a certain electrode parameter value in the geometric model is changed to establish different geometric models.First, according to the difference in electrode spacing, three geometric models were established, that is, when the electrode length is 12.5 mm, the electrode spacing is changed to 1.25 mm, 2.5 mm, and 4 mm. Then, based on the difference in electrode length, three other geometric models were established. When the electrode spacing was 1.25 mm, the electrode length was changed to 6 mm, 12.5 mm, and 20 mm.Taking into account the sensor structure and the symmetry of the exhaust pipe, in order to simplify the model and reduce the amount of calculation, only half of the model was built.

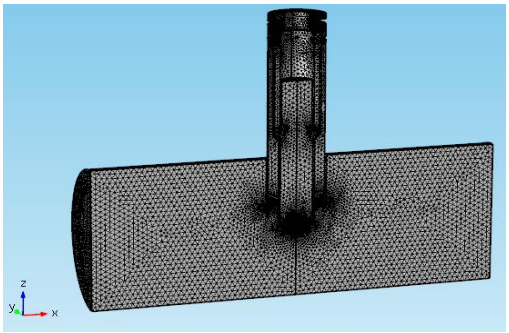

Fig. 2. Mesh model drawing of PM sensor coupling DPF.

After the geometric model of the sensor installed on the exhaust pipe is established, it needs to be meshed.The meshing module in COMSOL is used for meshing. Since the sensor is the main research object and its internal structure is complex, the sensor part is mainly divided by tetrahedron and encrypted. Figure 1 shows the grid division of the geometric model with an electrode spacing of 1.25 mm and an electrode length of 12.5 mm.

Select κ-ε turbulent flow model, steady-state electrostatic field model and fluid particle tracking model to establish a three-dimensional calculation model of the sensor.

The exhaust flow rate is based on the bench test results of the 186FA diesel engine. In the test, a PVC pipe with a diameter of 35 mm is selected for the exhaust pipe. The calculated exhaust flow rate varies from 5.7 m/s to 13.7 m/s.This article mainly studies the influence of sensor structure parameters on the movement of particulate matter under a certain exhaust flow rate. The exhaust flow rate of diesel engine is 13.7 m/s under 100% load at the rated speed of the diesel engine, and the exhaust pipe inlet flow rate is set to 13.7 m/s. In this article, it is assumed that the nature of the exhaust gas is constant, and the exhaust gas is regarded as an incompressible fluid, so only the relative value of the pressure is considered at the outlet of the exhaust pipe, and the pressure outlet boundary condition is set to 0. The numerical simulation input parameters are shown in Table 1.

Table 1. Input numerical parameters.

The parameter name	The numerical
Inlet flow velocity (*m/s*)	13.7
Particulate charge	-3, 0, 3
Particle diameter (*μm*)	0.1
The length of the electrode (*mm*)	6, 12.5, 20
Electrode gap (*mm*)	1.25, 2.5, 4
The electrode voltage (*V*)	500, 1000, 1500

4 Model validation

In order to verify the accuracy of the model, it is necessary to compare the simulation results with the test results. The 186FA single-cylinder diesel engine was selected for the test, and the engine speed was adjusted to 3600 r/min and the load was 100%. The Pitot static pressure tube is used to measure the radial distribution of the axial velocity at the outlet end of the exhaust pipe.The structure of the Pitot static pressure tube is shown in Figure 2.8. The Pitot tube is located in the middle position, and calculate the flow velocity

at the measuring point based on the difference between the total pressure and the static pressure.

Figure 3 is the velocity field distribution on the exhaust pipe section 40 mm away from the sensor center axis on the leeward side of the sensor obtained by numerical simulation. The velocity distribution of the horizontal axis and the vertical axis of the exhaust pipe is analyzed, and compare the simulation results with the velocity distribution obtained from the experiment.

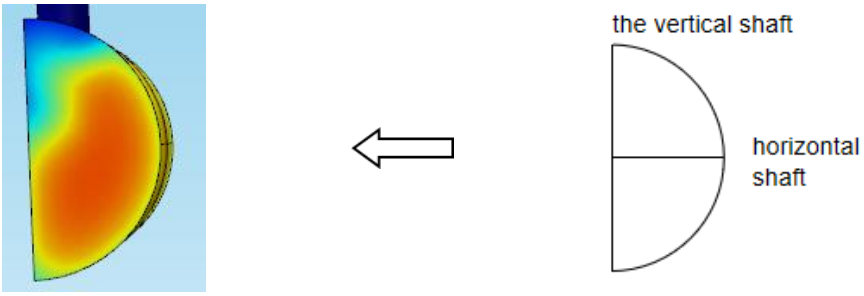

Fig. 3. Velocity distribution of the cross section of the exhaust pipe.

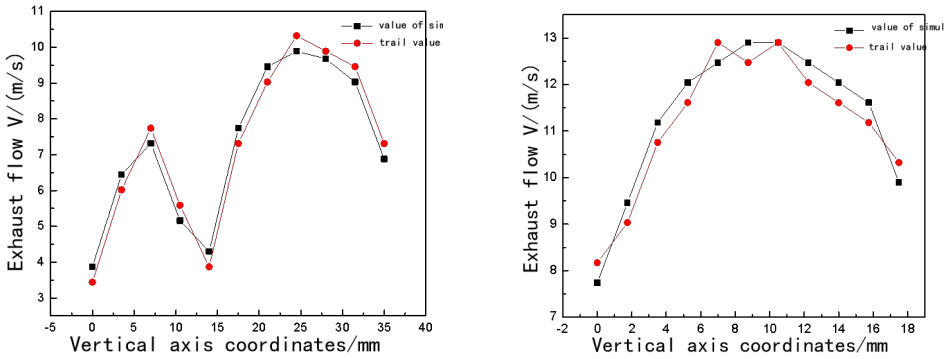

Fig. 4. The comparison drawing of simulated and experiment values.

5. Analysis of calculation results

5.1 Analysis of flow field simulation result

Macroscopically, the velocity field distributions on the central section of the sensor and the exhaust pipe under different electrode parameters are roughly similar.Therefore, this article only analyzes the velocity field distribution on the cross section of the sensor and the exhaust pipe when the sensor electrode spacing is 1.25 mm and the electrode length is 12.5 mm, as shown in Figure 5. It can be seen from the Figure that in the area of the exhaust pipe on the windward side of the sensor, the exhaust flow velocity distribution is relatively Table. When the exhaust moves to the sensor head, the flow section decreases, resulting in an increase in the exhaust flow velocity. When the exhaust gas flows through the sensor head and enters the area on the leeward side of the sensor, the area above the exhaust pipe

is blocked by the sensor, so the exhaust flow rate is small, and the area below the exhaust pipe has low resistance, and the flow velocity is higher, which is not much different from the inlet flow rate.Macroscopically, except for the obvious velocity gradient distribution in the sensor area, the flow velocity distribution in the exhaust pipe is relatively Table.

When the exhaust gas moves to the inlet of the windward side of the sensor, the flow rate of the exhaust gas is significantly reduced due to the obstruction of the sensor.The exhaust flow rate at the inlet of the windward side of the sensor has a clear gradient distribution. Due to the complex internal structure of the sensor and the effect of the baffle inside the sensor, the exhaust flow rate inside the sensor is significantly reduced and is roughly stable in the range of 0 to 4m/s.

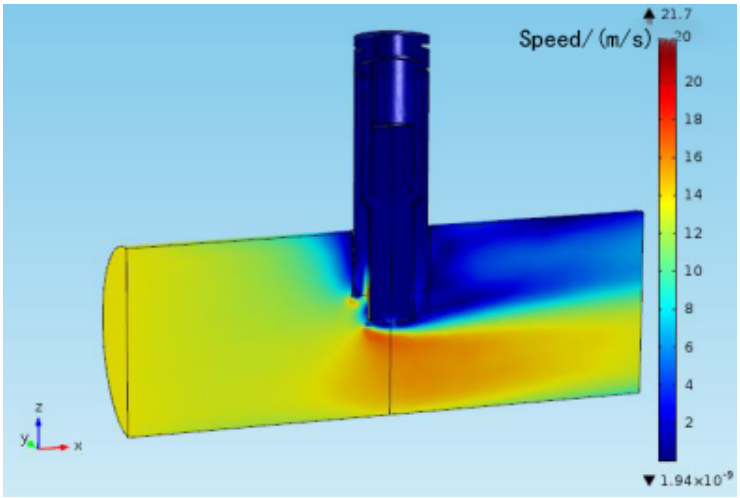

Fig. 5. Exhaust velocity distribution in the sensor and the exhaust pipe.

5.1.1 Distribution of flow field in sensor with different electrode spacing

Figure 6 is an enlarged view of the velocity vector distribution of part of the sensor when the sensor electrode length is 12.5 mm, and the electrode spacing is 1.25 mm, 2.5 mm, and 4 mm. The velocity in some areas is not displayed because the exhaust flow rate in this area is greater than 1.5 m/s.Under the action of the venturi principle, the exhaust gas will flow upwards into the protective space outside the sensor. During the upward movement, due to the further reduction of the cross-sectional area, the exhaust flow rate will increase to a certain extent, and then stabilize and form a speed gradient distribution.As the electrode spacing gradually increases, the exhaust gas flow rate in the outer protection zone gradually increases, and the velocity gradient distribution becomes more obvious.

It can be seen from Figure 6 that under the three electrode spacings, the exhaust gas flow rate in the concentration test area is relatively stable, and no obvious velocity gradient distribution is seen.As the electrode spacing gradually increases, the flow rate of the exhaust gas in the sensor concentration test area gradually decreases.When the exhaust gas flow into the concentration test area is the same, the electrode spacing gradually increases, and the exhaust gas flow cross-sectional area increases, so the exhaust gas flow rate decreases, and the decrease of the exhaust gas flow rate will also cause the movement speed of the particles to decrease, which will affect the performance of the sensor.

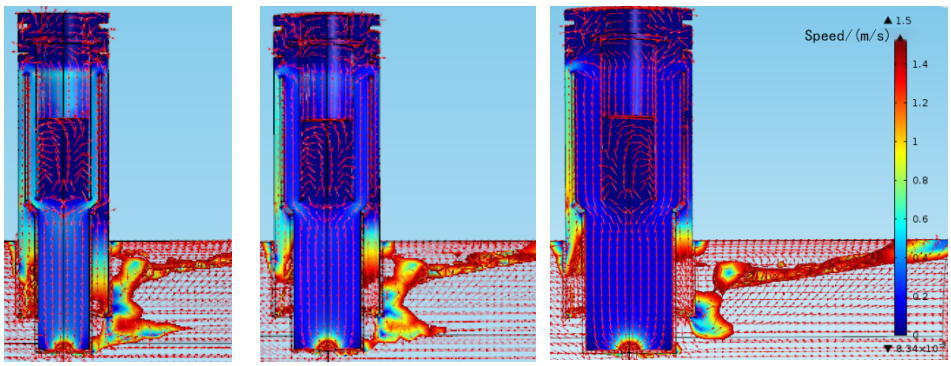

(a) 1.25 mm (b) 2.5 mm (c) 4 mm

Fig. 6. Velocity vector distribution of the exhaust in sensors with different electrode spaces.

5.1.2 Flow field distribution in the sensor under different electrode lengths

Figure 7 shows the velocity vector distribution diagram of the sensor when the sensor electrode spacing is 1.25 mm, and the electrode length is 6 mm, 12.5 mm, and 20 mm.It can be seen from the Figure that the change of electrode length has little effect on the velocity field distribution at the entrance of the sensor, and there is little difference in the distribution of the exhaust velocity gradient at the entrance of the sensor under the three electrode lengths.When the exhaust gas continues to move upward from the sensor inlet and moves to the necking area of the outer protective space, as the length of the electrode gradually decreases, the velocity gradient distribution of the exhaust gas in this area becomes more obvious. This is mainly because the length of the electrode is reduced, and the time for the exhaust to move up to the labyrinth shoulder from a higher flow rate becomes shorter, and it will be blocked by the labyrinth shoulder in advance.Taking a sensor with an electrode length of 6 mm as an example, when the exhaust gas moves in the outer protective space area, the flow rate is not yet stable and is blocked by the shoulders, causing the exhaust flow rate to decrease significantly, forming a more obvious velocity gradient distribution, which is not conducive to the stable flow of exhaust gas in the sensor, and has a certain impact on the flow stability of particulate matter in the sensor.With the gradual increase of the electrode length, the flow rate of the exhaust gas in the outer protective space and the concentration test interval is gradually reduced. When the particle flow rate is too low, it will not only cause the particles to accumulate in the sensor, which will have a certain impact on the normal operation of the sensor, but also will cause the charge transfer rate in the concentration test interval to decrease, prolong the response time of the sensor to particles and reduce the sensitivity of the sensor.

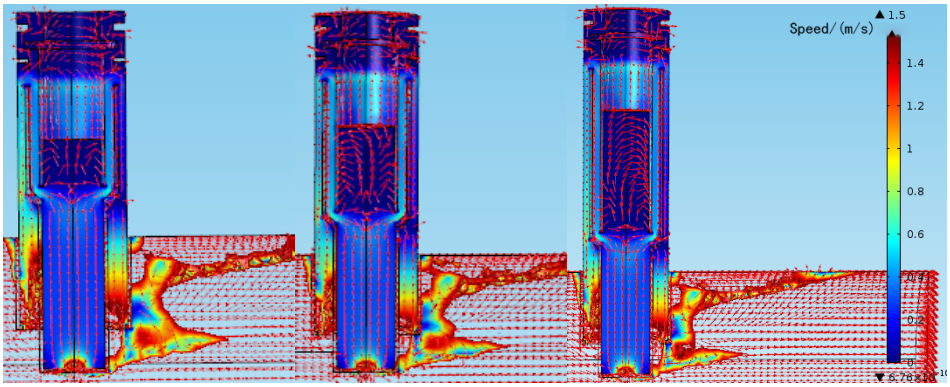

(a) 6mm (b) 12.5mm (c) 20mm

Fig. 7. Velocity vector distribution of the exhaust in sensors with different electrode lengths.

5.2 Analysis of electric field simulation results

The structural parameters of the sensor will have an important influence on the electric field distribution area and the intensity of the electric field. Figure 8 shows the electric field intensity distribution on the cross section of the sensor concentration test area when the high-voltage electrode voltage is 1000 V and the sensor is at 1.25 mm, 2.5 mm, and 4 mm electrode spacing.The color change of different areas indicates the change of the electric field intensity, and the direction of the red arrow represents the direction of the electric field intensity. It can be seen from the Figure that the electric field in the sensor concentration test area is a non-uniform electric field, and the electric field intensity varies everywhere.

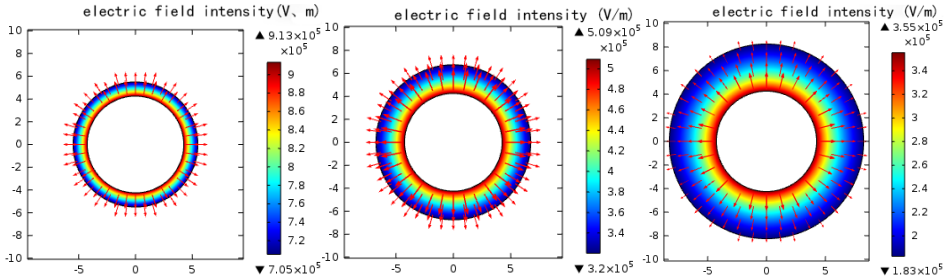

(a) 1.25mm (b) 2.5mm (c) 4mm

Fig. 8. Distribution of electrode field intensity in the sensors with different electrode spaces.

The intensity of the electric field at any point in the concentration test area is related to the radial distance from the point to the surface of the high-voltage electrode. The greater the radial distance, the smaller the electric field intensity. The electric field intensity of the surface area of the high-voltage electrode is the largest, and the electric field intensity of the surface area of the grounding electrode is the smallest; the direction of the electric field strength at any point is divergent from the high-voltage electrode to the grounding electrode along the radial direction at that point.

The change curve of the electric field intensity in the sensor with different electrode spacing along the radial direction is shown in Figure 9. Under the three electrode spacings, the electric field intensity in the sensor decreases with the increase of the radial distance, and the larger the electrode spacing, the slower the downward trend. At the same time, as

the electrode spacing increases, the average electric field intensity in the sensor decreases, and both the highest electric field intensity and the lowest electric field intensity decrease to a certain extent.

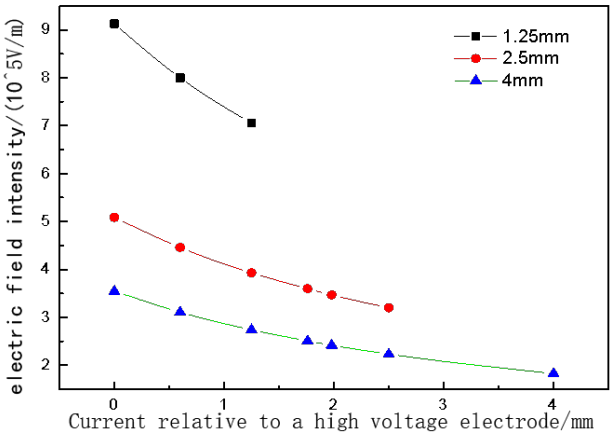

Fig. 9. Variety of electrode field intensity with the radial distance in the sensor.

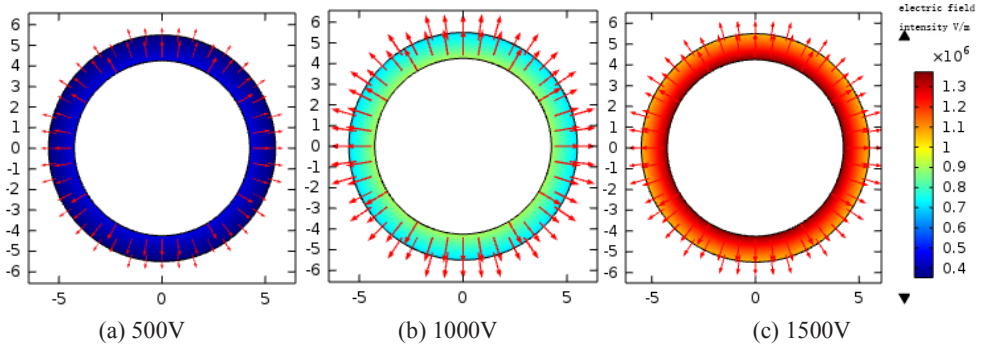

Fig. 10. Distribution of electrode field intensity in the sensor with different electrode voltage.

Figure 10 shows the electric field intensity distribution on the cross section of the sensor concentration test area when the sensor electrode spacing is 1.25 mm and the high-voltage electrode voltage is 500 V, 1000 V, and 1500 V. As the electrode voltage increases, the electric field intensity gradient distribution in the sensor becomes more obvious.

Under the three electrode voltages, the change curve of the electric field intensity in the sensor along the radial direction of the sensor is shown in Figure 11.It can be seen from Figure 11 that the larger the electrode voltage, the smaller the average electric field intensity in the sensor, in the same sensor, the electric field intensity gradually decreases from the surface of the high-voltage electrode to the ground electrode along the radial direction of the sensor, and the smaller the high-voltage electrode voltage, the slower the change of electric field intensity.

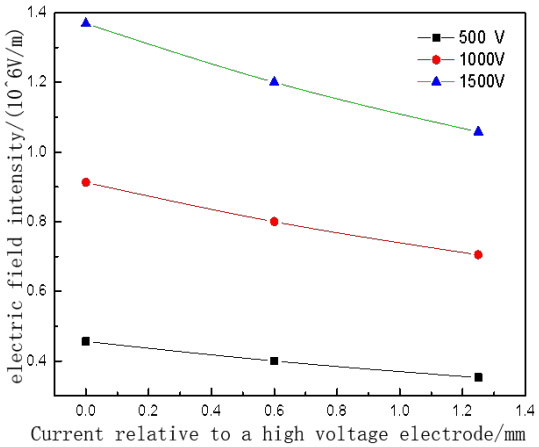

Fig. 11. Variety of electrode field intensity with the radial distance in the sensor.

6 Conclusion

The sensor electrode spacing, electrode length, electrode voltage were changed and numerical simulation calculations were carried out. The flow field distribution and electric field distribution in the sensor under different electrode structure parameters are simulated, and the influence of the sensor structure parameters on the movement and displacement of particles is analyzed, and the simulation results are verified through experiments, and the following conclusions are drawn:

When the exhaust gas moves to the area near the sensor, the exhaust flow rate will produce an obvious velocity gradient distribution. The exhaust flow rate in the area directly in front of and behind the sensor is significantly reduced, while the exhaust flow rate in the area directly under the head of the venturi tube of the sensor increases to a certain extent. The exhaust gas flow rate inside the sensor is relatively low, roughly in the range of 0 to 4 m/s.

As the electrode spacing increases, the velocity distribution gradient of the exhaust gas at the entrance of the sensor increases, and at the same time the exhaust gas flow rate decreases in the sensor concentration test interval; the longer the electrode length, the more stable the velocity distribution of exhaust gas in the sensor, and the lower the exhaust gas flow rate.

In the case of keeping the voltage of the high-voltage electrode constant, the increase of the electrode spacing will result in the decrease of the electric field intensity in the sensor. The farther the distance between any point in the sensor and the high-voltage electrode, the smaller the electric field intensity at that point. The direction of the electric field intensity is from the high-voltage electrode to the ground electrode along the radial direction of the sensor; When the electrode spacing is constant, the higher the electrode voltage, the greater the average electric field strength; the increase of the electrode spacing or the decrease of the electrode voltage will make the change of the electric field strength in the sensor tend to be slow.

This research was funded by National Natural Science Fund of China(51876085) and Open Fund of National Key Laboratory for Internal Combustion Engine and Dynamic System in China (skler-202105).

References

1. Feng Fei. Advanced diesel engine technology should be an important part of China's automobile energy strategy[R]. Executive report of the Industrial Economic Research Department of the Development Research Center of the State Council, 2006.Zhang Zongfa, Wu Jiannin, Wei Wenqiu. Discussion on the Development Trend of Future Automotive Engines [J]. Automotive Industry Research, 2012(8): 9-13.
2. Zhang Zongfa, Wu Jianian, Wei Wenqiu. Talking about the future development trend of automotive engines[J]. Automotive Industry Research, 2012(8): 9-13.
3. Ministry of Environmental Protection, General Administration of Quality Supervision, Inspection and Quarantine. Light-duty vehicle pollutant emission limits and measurement methods (China Phase 5): GB 18352.5-2013[S]. Beijing: China Environmental Science Press, 2013.
4. Ministry of Environmental Protection, General Administration of Quality Supervision, Inspection and Quarantine. Emission Limits and Measurement Methods for Light Vehicle Pollutants (China stage 6): GB 18352.6-2016[S]. Beijing: China Environmental Science Press, 2016.
5. the environmental protection department of the state administration of quality supervision, inspection and quarantine. Automotive compression ignition, fuel gas spark ignition engine and vehicle emission pollutant emission limits and discharge method (China Ⅲ, Ⅳ, Ⅴ phase) : GB 17691-2005 [S]. Beijing: China Environmental Science Press, 2005.
6. Thorsten Ochs, Henrik Schittenhelm, Andreas Genssel, et al. Particulate matter sensor for on board diagnostics (OBD) of diesel particulate filters(DPF)[C]. SAE International, 2010-01-0307, 2010.
7. D. Grondin, A. Westermann, P. Breuil, et al. Influence of key parameters on the response of a resistive soot sensor[J]. Sensors and Actuators B: Chemical, 2016(236): 1036-1043.
8. S.Amanatidis, L.Ntziachristos, Z.Samaras, K.Janka, J.Tikkanen, Applicability of the Pegasor particle sensor to measure particle number, mass and PM emissions[C]. SAE Technical Papers, 2013-24-0167, 2013.
9. EmiSense develops next-generation emissions sensors[EB/OL]. http://emisense.com/.
10. J. Steppan, B. Henderson, K. Johnson, et al. Comparison of an on-board, real-time electronic PM sensor with laboratory instruments using a 2009 heavy-duty diesel vehicle[C]. SAE International, 2011-01-0627, 2011.
11. K. Almendingo, B. Henderson, A. Rodhasami, et al. Sensors for measuring particulate matter accumulation and charge loss [P], China: CN103688161A, 2014.03.26.